Source reconstruction of clinical resting-state EEG reveals differences in power and functional connectivity in children with developmental dyslexia

David Garnica-Agudelo
david.garnica@med.uni-goettingen.de

Universitätsmedizin Göttingen https://orcid.org/0000-0002-1527-2290

Stuart D.W. Smith
Great Ormond Street Hospital for Children: Great Ormond Street Hospital For Children NHS Foundation Trust

Daniel van de Velden
Universitätsmedizin Göttingen: Universitatsmedizin Gottingen

Christina Stier
Universitätsmedizin Göttingen: Universitatsmedizin Gottingen

Knut Brockmann
Universitätsmedizin Göttingen: Universitatsmedizin Gottingen

Sascha Schroeder
Georg-August-Universität Göttingen: Georg-August-Universitat Gottingen

Nicole E. Neef
Universitätsklinikum Göttingen: Universitatsmedizin Gottingen

Niels K. Focke
Universitätsmedizin Göttingen: Universitatsmedizin Gottingen

Research

Keywords: Dyslexia, Electroencephalography, Functional Connectivity, Brain Network, Source reconstruction, Reading, Spelling

Posted Date: May 23rd, 2023

DOI: https://doi.org/10.21203/rs.3.rs-2895521/v1

Abstract

Background: Developmental dyslexia is a neurodevelopmental disorder characterized by significant difficulties in reading and spelling. Despite lacking routine neuroimaging markers for dyslexia, recent resting-state electroencephalography (EEG) studies have detected atypical functional connectivity in children with dyslexia compared to controls. These methods are based on measures of EEG data at a sensor-level, but it remains unclear if routine clinical resting-state EEG can be used to detect source-level differences in power or functional connectivity (FC) between children with dyslexia and controls. It is also unknown if differences in these EEG metrics correlate with difficulties in reading and spelling.

Methods: Using retrospective data, we investigated the source-reconstructed power and FC of 70 children with recently diagnosed dyslexia and 50 typically developing controls. We analyzed 50 seconds of awake resting-state routine clinical EEG in five frequency bands (1-29 Hz) using power, imaginary part of coherency (ImCoh), and weighted phase lag index (wPLI). Additionally, we calculated correlations between power or FC and IQ, reading, and spelling performance.

Results: Children with dyslexia had a decrease in theta FC in left temporo-parieto-occipital regions and an increase in alpha FC in left fronto-temporo-parietal regions. A decrease of theta FC was observed for right parieto-occipital regions and an increase of alpha FC in right inferior fronto-temporal regions. Furthermore, children with dyslexia demonstrated lower power in delta and theta within the left parieto-occipital regions. An age-stratified sub-analysis indicated that children with dyslexia in 5th-8th school grades exhibit greater alpha FC mainly in left fronto-temporo-parietal regions. Finally, lower scores in spelling showed a positive and significant association to theta power within left parieto-occipital regions in dyslexia.

Conclusions: Significant group differences in power and FC in the theta-alpha range in left cortical language and visual regions, as well as in multiple resting-state networks (RSNs), suggest abnormal oscillations as a pathophysiological sign of dyslexia reading and spelling deficits. These findings demonstrate the potential of source-reconstructed clinical routine EEG data to inform clinicians about brain network alterations in neurodevelopmental disorders such as dyslexia.

Background

Developmental dyslexia (DD) is a neurodevelopmental disorder defined by significant difficulties in reading and spelling, despite adequate intelligence, schooling, and mathematical skills[1–4]. Its etiology is considered multifactorial, with origins at the genetic, neural, and cognitive levels[5]. Between 1.9% and 10% of the English and German speaking children are estimated to have DD[6–8], and many of them experience academic underachievement[9,10]. Although a comprehensive explanation for the cognitive difficulties in DD has remained elusive, recent research with neuroimaging and electroencephalography (EEG) has revealed functional abnormalities as possible neurobiological correlates. Studies using functional resonance imaging (fMRI) with DD speakers of multiple languages have shown lower activation in left temporo-parietal and occipito-temporal regions during reading and rhyming tasks, which presumably implies a phonological speed deficit and explains their difficulties in both lexical recognition and serial sublexical decoding[5, 11–17]. Similarly, magnetoencephalography (MEG) studies with language tasks found atypical auditory neural synchronization of delta, alpha, and beta oscillations in children with DD, confirming a deviant neural processing of syllabic and phonemic information[18–20], and an atypical entrainment to speech information[21]. This evidence supports the temporal sampling theory, which proposes an atypical speech development trajectory for DD, where the discrimination of acoustic speech signals (amplitude envelope) and the associated accuracy of the neural oscillatory phase alignment (entrainment) is atypical at rates < 10 Hz[22,23]. These differences constrain speech and reading development, as the speech cues perception is impaired since infancy, and the phonological representations for visual word forms are learned differently[18, 21–24]. Additionally, a magnocellular theory has proposed that the magnocellular system is impaired in persons with DD, affecting the spatio-temporal parsing of visual inputs within the visual system, and constraining the development of the letter-word recognition and sublexical processing[25–29]. Therefore, the magnocellular theory extends a temporal sampling deficit for phonological stimuli to the auditory-visual integration required during the reading development[25–27].

Further, studies in rest have demonstrated FC changes not restricted to the language network, supporting a disrupted phonological processing and an atypical phonological-visual integration. A meta-analysis of resting-state fMRI (rs-fMRI) studies revealed that intra-connectivity within resting-state networks (RSNs) (limbic, somatomotor, ventral attention, dorsal attention, visual, DMN, and fronto-parietal) is correlated with reading skill, and that FC abnormalities in children with DD localize onto the hub areas that connect RSNs[30]. Two whole-brain rs-fMRI analyses found decreased FC along the visual pathway and between visual and prefrontal regions, increased FC between reading-related areas (fusiform gyrus, inferior temporal gyrus, middle temporal gyrus, and inferior parietal lobe) and areas of the default mode network (DMN), reduced FC to the visual word form area (VWFA), and reduced FC between the left inferior frontal gyrus and left posterior temporal areas (fusiform gyrus, inferior temporal gyrus, middle temporal gyrus, superior temporal gyrus)[31,32]. Studies with EEG in rest have demonstrated lower information integration and connectivity in the theta and beta bands[33,34], lower alpha power in parieto-temporo-occipital regions in correlation to poorer reading time of pseudowords, and higher effective connectivity in all the frequency bands from the left calcarine sulcus to the right postcentral gyrus, left paracentral gyrus, right angular gyrus, and right supplementary motor[35,36]. Lastly, investigations with MEG in rest found significantly reduced global network efficiency, temporal correlations between sensors of the left temporo-parietal region and the rest of the sensors in the beta band, and significantly increased phase-to-amplitude coupling variability between left fronto-temporo-occipital sensors and their corresponding right hemisphere sensors[37–39].

In summary, children with DD show consistently neurobiological features defined by atypical FC and information exchange comprising RSNs, but also an atypical recruiting of the language and visual networks[5,21,30,37]. Hence, it is relevant to investigate possible EEG signatures of DD at rest, using source reconstruction of cortical sources[40,41], and the Desikan-Killiany[42] and Yeo[43] atlases to attribute the reconstructed data to anatomical regions and functional networks. Accordingly, our main objective was to investigate if, compared to controls, children with DD show significant power and FC differences in source reconstruction of low-density routine resting-state EEG data. Secondarily, we evaluated if power and FC differences are significantly related to performance in phonological awareness, reading, and spelling tests. We hypothesize that *1)* children with DD exhibit significant differences in power and FC in vertices not restricted to the reading and language networks; and 2*)* a significant positive association between power or FC and performance in subtests involving reading and spelling.

Methods

Participants

We included scalp EEG and psychological testing data in a retrospective study design. The measurements were carried out for children that attended the Interdisciplinary Center for Children with Developmental Disabilities and Severe Chronic Disorders, University Medical Center of Göttingen, Germany, between 2008 and 2022.

Seventy children were selected from a pool of 330 children whose main diagnosis was DD. The diagnosis followed the International Classification of Diseases (ICD-10) and the Diagnostic and Statistical Manual of Mental Disorders, 5th Ed. (DSM-5)[3] criteria, namely, performance in psychological tests more than 1.2 standard deviations (SD) below the mean. Inclusion to the DD group required clinically normal EEG and brain MRI (when available). Children with secondary diagnoses of attention deficit with/without hyperactivity (ADD/ADHD), dyscalculia, central auditory processing disorder, mild expressive speech disorder, developmental coordination disorder, anxiety disorder, or childhood emotional disorder were included as these commonly coexist with DD[44–46]. We excluded children with a primary diagnosis of intellectual disabilities (IQ < 80), perinatal morbidities, prematurity (term ≤ 28 weeks of gestation), epilepsy, generalized developmental disorders, tumors, autoimmune diseases, stroke, psychiatric diagnoses, autism spectrum disorder, and migraine.

Fifty hospital outpatients were selected as typically developing controls. These children had been referred for the assessment of cephalgia, vertigo, syncope, social behavior difficulties, or sleep difficulties (if not deemed clinically significant). Consultant neurophysiologists reported all their EEGs as normal. Pediatric neurologists found these children to have a normal developmental profile with no special schooling needs. Hence, none of the control children had neuropsychological assessment. Children with abnormal EEG (interictal epileptiform discharges – IEDs–, slowing or asymmetry), migraine, ID, developmental disorders, significant school performance difficulties, ADD/ADHD, and convulsive concussion were excluded. All children were German native speakers, and in the first to eighth grade of schooling. Children with DD and controls were matched for age and sex. Finally, children with regular medications were included, e.g. magnesium for cephalgia, but the remainder of children were naïve for psychiatric and anti-seizure medications.

Electroencephalography

The EEG recordings were done at rest and with eyes closed, using the local clinical protocol. The EEG data contained 19 scalp channels (international 10–20 system: FP1, FP2, F3, F4, F7, F8, Fz, C3, C4, Cz, P3, P4, Pz, T3, T4, T5, T6, O1, O2), two earlobes' re-reference channels (A1, A2), and one electrocardiography channel (ECG). It was exported from a Natus® NicVue (version 3.06)/Nicolet EEG (version 5.92.1) system, with a sampling frequency of 250 Hz, 30 Hz low-pass filter, and 0.5 Hz high-pass filter. Given the known rater-dependency of clinical EEG scoring, we carried out a strict re-review. All EEGs were re-scored independently by the main researcher (D.G.) and one EEG-experienced clinical physiologist (S.S.) in a two-stage process. First, automatic detection of IEDs using the Persyst® Spike Detector P14 (Persyst, San Diego, California, USA; non-clinical use, Version 14, Rev. D) was performed. Second, visual inspection and interpretation of the EEG were carried out to confirm or discard IEDs grapho-elements, identify and keep awake trials, reject drowsiness trials, and detect other abnormalities such as background asymmetries or slowing. Only segments where both raters agreed that the EEG data was normal were included into the further analyses.

EEG signal processing

Our EEG pipeline included the following preprocessing steps: EEG data downsampling to 250 Hz, epochs' length definition, events assignment, clean epochs selection, manual artefact rejection, independent component analysis (ICA), and vigilance scoring. These procedures were performed using Fieldtrip (fieldtriptoolbox.org/)[47] running in Matlab (version 9.5, update 7, R2018b, Mathworks Inc.). The reference (A1, A2) and ECG signals were removed leaving 19 scalp channels. For each patient, the EEG data were cut into epochs of 10 seconds in length. ICA was performed to identify and exclude components related to cardiac artefacts and ocular movements. Vigilance was rated following the sleep-scoring criteria of the American Academy of Sleep Medicine[48]. Five epochs of processed and awake data (50 seconds) per subject were then randomly selected for further analyses.

Source reconstruction

The retrospective design precluded the collection of structural MRI data. Thus, we used an MRI template obtained from 225 normal-control adults originally scanned with 3T T1 + FLAIR, whose images were non-linearly transformed to an MNI-space similar template using ANTs/SyN transformations[49]. This template image was then passed through Freesurfer[50] and SUMA[51] to yield a canonical head model and, using standard 10/20 electrode positions, a canonical lead field. This procedure produced 1169 common vertices per hemisphere as EEG source points, with vertex-based correspondence across subjects. For each vertex of the cortical mesh, a lead field matrix was calculated. Source reconstruction was done using a beamformer method (dynamic imaging of coherent sources[40]), and it was performed separately for every frequency band and every EEG metric analyzed. Other referenced technical details of the source reconstruction can be found in a previous publication[52].

Spectral power

An absolute spectral power and cross-spectral density analysis was carried out first on the EEG sensor level using the Fast Fourier Transformation (FFT) in Matlab. After beamforming, the spectral power analysis was performed at the source level, implementing FFT and Fieldtrip. In both sensor- and source-level analyses, the relative power values were obtained for five frequency bands: delta (2 ± 2 Hz), theta (6 ± 2 Hz), alpha (10 ± 2 Hz), beta1 (16 ± 4 Hz), and beta2 (25 ± 4 Hz). The gamma frequency is typically more influenced by muscle artefacts in children than in adults, and for this reason a low-pass filter was applied to exclude it from analysis, following other resting-state EEG studies[33,34,53].

Functional connectivity analyses

To test the first hypothesis, we calculated the imaginary part of coherency (ImCoh) and the weighted phase lag index (wPLI), as undirected measures of the FC strength between EEG signals[54,55]. ImCoh is a measure that aims at detecting synchronization between brain signals by reducing the impact of volume conduction[54,56]. It is assumed that neuronal synchronization of distant sources has a time-lag and, thus, instantaneous synchronization effects (volume conduction) are not biologically informative. WPLI detects changes in phase synchronization between brain regions by estimating the phase leads and lags between two timecourses[55]. This metric is weighted by the magnitude of the imaginary component of the cross-spectrum and, similarly to ImCoh, it is less susceptible to volume conduction and synchronous noise[54–56]. Both methods have been applied in resting-state EEG and MEG to study healthy subjects[57], children or adults with epilepsy[58–64]. Both ImCoh and wPLI analyses were performed in Matlab/Fieldtrip, for the five frequency bands of interest.

After beamforming, ImCoh and wPLI values were calculated for every frequency band and between all pairs of vertices. As a result, an individual, symmetrical, and weighted matrix was constructed for every frequency band. For FC, the weights and links of each vertex were averaged to obtain overall connectivity strength per vertex, and both power and FC values were averaged across all vertices to produce a global value per subject.

Statistical analyses

Group differences in power and FC were analyzed using Permutation Analysis of Linear Models (PALM), a nonparametric statistical tool (fsl.fmrib.ox.ac.uk/fsl/fslwiki/PALM). To contrast the data at the global and vertex-based levels, we ran two one-sided comparisons (*Dyslexia < Controls*, *Dyslexia > Controls*). A general linear model (GLM) was computed for every permutation, with power and FC metrics as dependent variables. Age and sex were included in the GLMs as demeaned regressors. This process was repeated 5,000 times with shuffled subjects and tail approximation, resulting in empirical distributions from which *p*-values were obtained. In the vertex-based analysis, a correction for multiple comparisons on cluster level using threshold-free cluster enhancement (TFCE) was implemented[65]. Family wise error correction (FWE) was performed for *p*-values within each group contrast. *P*-values were log-transformed and are indicated as $-\log_{10}(p\text{-value})$. We used a significance threshold of 1.3 ($p \leq 0.05$). *P*-values per vertex and EEG metric were labeled using the Desikan-Killiany atlas, which allowed an analysis of the vertices corresponding to anatomical regions[42].

In addition, a subanalysis was carried out to investigate group differences at the network-level using the Yeo atlas[43]. To this end, the power and FC data were resampled using the Yeo 7-network atlas and rerunning PALM for the power/FC values per RSN as dependent variables. Two one-sided comparisons (*Dyslexia < Controls, Dyslexia > Controls*) were performed, a GLM was computed for every permutation, age and sex were included as demeaned regressors, and the process was repeated 5,000 times with shuffled subjects and tail approximation. *P*-values were obtained from the resulting empirical distributions and TFCE and FWE corrections were applied for each group contrast, with a significance level of 1.3 ($p \leq 0.05$) and a log-transformation of $-\log_{10}$(*p*-value).

Finally, to test for possible different EEG signatures due to development in the whole DD sample, vertex-based subanalyses were carried out by dividing the DD sample into subgroups of 1st -4th school grades and 5th -8th school grades and comparing them to sex- and age-matched controls. Again, power and FC metrics were used as dependent variables in PALM, and the same procedure was applied. TFCE- and FWE-corrected *p*-values per contrast were labeled using the Desikan-Killiany atlas[42].

Neuropsychology

From 70 children with DD, 68 different children were assessed with the German versions of Wechsler Intelligence Scales (Hamburg-Wechsler-Intelligenztest für Kinder, HAWIK-IV; Wechsler Intelligence Scale for Children, Fourth Edition, WISC-IV; Wechsler Intelligence Scale for Children, Fifth Edition, WISC-V). Reading was tested using Salzburger Lesetest (Zweite Version –SLRT-II–) or Zürcher Lesetest (Zweite Version –ZLT-II–). Lastly, spelling was assessed with modified versions of Weingartener Grundwortschatz Rechtschreib-Tests (WRT+, 1st -4th grades) or with Hamburger Schreib-Probe (HSP+, 5th -8th grades). Internationally, these German reading tests are equivalent to the one-minute Test of Word Reading Efficiency–Second Edition (TOWRE-2)[66]. The Germanic spelling tests are highly comparable to the spelling-punctuation dimensions of the Test of Written Language 4[67] and Test of Written Spelling 4th -5th grades[68].

We analyzed subtests of the Wechsler including full-scale intellectual quotient (FSIQ), verbal comprehension index (VCI), visual-spatial index (VSI, from WISC-V), fluid reasoning index (FRI, from WISC-V), working memory index (WMI), and the processing speed index (PSI). The *correct words* and *correct pseudowords* from SLRT-II were considered, which evaluated the number of correct words or pseudowords read in a minute. From ZLT-II were taken *words reading*, *pseudowords reading*, and *reading of text sections*, which evaluated the reading of high-frequency words, low-frequency words, and segments of text, in up to 2 minutes per subtest. From WRT and HSP, the *spelling* subtests were included, which assessed the number of correctly written words. Next, all subtests from IQ, reading, and spelling tests were converted from percentage ranks (PRs) to z-scores. By definition, z-scores have a mean of zero and an SD of 1, with a significant deficit indicated by a z-score ≤ -2 (PR ≤ 2.3) and poor performance indicated by a z-score between – 1 and – 1.9 (PR 16 – 2.3)[69]. The effect of age was controlled in this conversion through the cut-offs per school year provided by the tests´ scoring manuals[70–73].

Correlation analyses

To calculate correlations, single z-scores and power/FC values were taken for every child with DD. As children were assessed with different cognitive tests, power/FC values were taken only for those who were assessed with each test (Table 2). Knowing that tests have distinct subtests, we used z-scores of subtests that measure the same cognitive process. Hence, we used FSIQ, VCI, WMI, and PSI from WISC-IV/HAWIK-IV and WISC-V (to correlate FSIQ, VCI, WMI, and PSI); words reading and pseudowords reading from SLRT-II and ZLT-II (to correlate words reading and pseudowords reading); and spelling from WRT and HSP (to correlate spelling). As SLRT-II does not evaluate the reading of text segments, a correlation of this cognitive process was assessed using z-scores from ZLT-II.

The relationship between power/FC values and z-scores was tested by calculating Spearman rank correlations. This coefficient was chosen due to the different tests used and the different number of children tested retrospectively. Additionally, partial rank correlations were calculated to control for age. Because cognitive performance data from controls was unavailable and we aimed to focus the analysis on regions where DD patients differed from controls, masks of the significantly different vertices between children with DD and matched controls were created. Using one mask per contrast, the raw power/FC values were selected, that is, the values obtained before the group comparison with PALM but after the source-reconstructed power/FC calculation. Next, correlations were calculated in two spatial levels: *1*. as a global average per subject for all in-mask vertices; and *2*. per region of the Desikan-Killiany atlas for all in-mask vertices (for all regions with > 10 vertices in the analysis mask). Correlations were corrected from multiple comparisons using FDR[74]. This was applied to the number of frequency bands at the global level and to the number of significantly correlated regions at the regional level.

Results

Clinical and demographic data

Children with DD (mean age = 9.23, SD = 1.5, min = 7.02, max = 13.83) and controls (mean age = 9.54, SD = 1.53, min = 6.98, max = 13.58) were group matched for age and sex. A Chi-Square test did not demonstrate significant differences between these variables (*p*(age) = 0.56, *p*(sex) =

0.28). The average time between EEG and psychological tests was 1.81 months (SD = 2.16). Table 1 summarizes the demographic, academic, and diagnostic information from both groups.

Table 1
Demographic and clinical data for dyslexic children and healthy controls.

	Dyslexia		**Controls**	
	M(SD)	**%**	**M(SD)**	**%**
N	70		50	
Sex(M/F)	49/21	70/30%	31/19	62/38%
Age (years)	9.23(1.51)		9.54(1.53)	
School grades	1–2	26(37.14%)	1–2	18(36%)
	3–4	32(45.71%)	3–4	20(40%)
	5–6	10(14.28%)	5–6	10(20%)
	7–8	2(2.86%)	7–8	2(4%)
Comorbidities	ADD/ADHD	11(15.71%)	Chronic cephalgia	30(60%)
	Expressive speech disorder	8(11.43%)	Vertigo	9(18%)
	Central auditory processing disorder (CAPD)	2(2.86%)	Chronic nausea/vomiting	3(6%)
	Developmental coordination disorder	1(1.43%)	Syncope	8(16%)
	Dyscalculia	2(2.86%)	Social behavior difficulties	1(2%)
	Dysgraphia	6(8.57%)	Sleep difficulties	2(4%)
	Childhood emotional disorder	4(5.71%)	Childhood emotional disorder	1(2%)
	Anxiety disorder	3(4.29%)	Anxiety disorder	2(4%)
	Adjustment disorder	3(4.29%)		

Cognitive results

Children with DD showed normal performance in all IQ subtests, but significantly lower performance in all the reading and spelling subtests (≤ 1.2 SD). Details are given in Table 2.

Table 2
Z-scores of patients with dyslexia in IQ, reading, and writing tests.

Whole-sample				1st-4th school classes		5th-8th school classes	
Test	**Subtest**	***n***	**Mean(SD)**	***n***	**Mean(SD)**	***n***	**Mean(SD)**
WISC-IV or HAWIK-IV	FSIQ	56	-0.11(0.64)	47	-0.18(0.60)	9	-0.28(0.82)
	VCI		0.03(0.74)		-0.02(0.76)		0.29(0.72)
	PRI		0.27(0.70)		0.17(0.68)		0.80(0.67)
	WMI		-0.52(0.74)		-0.55(0.69)		-0.39(1.09)
	PSI		-0.21(0.83)		-0.30(0.88)		0.18(0.37)
WISC-V	FSIQ	12	-0.31(0.55)	9	-0.38(0.59)	3	-0.09(0.61)
	VCI		0.14(0.66)		-0.02(0.73)		-0.60(0.24)
	VSI		-0.28(0.61)		-0.21(0.59)		-0.49(0.27)
	FRI		0.07(0.53)		0.00(0.50)		0.27(0.77)
	WMI		-0.86(0.98)		-0.76(1.11)		-1.15(0.77)
	PSI		-0.39(0.64)		-0.40(0.71)		-0.38(0.65)
SLRT-II	Correct words	23	-1.78(0.44)	16	-1.75(0.49)	7	-1.83(0.38)
	Correct pseudowords		-1.65(0.45)		-1.58(0.48)		-1.76(0.42)
ZLT-II	Words reading	37	-1.23(1.32)	33	-1.32(1.35)	4	-0.36(0.84)
	Pseudowords reading		-1.41(1.44)		-1.41(1.41)		-1.29(2.03)
	Text segments		-1.57(1.23)		-1.72(1.10)		-0.26(1.76)
WRT	Spelling	57	-1.67(0.82)	53	-1.63(0.67)	4	-1.62(0.67)
HSP	Spelling	6	-1.88(0.32)	0	–	6	-1.88(0.34)

Spectral power at sensor space and source space

Power spectra at the sensor-level indicates a dissimilar distribution between DD and controls (Fig. 1A). After source reconstruction, power averages from all vertices reveal a significant decrease in theta band ($p = 0.041$, Cohen´s $d = 0.34$)(Fig. 1B).

Functional connectivity – global analysis

Figure 2 Violin plots of global FC metrics comparing children with DD and controls, after source-level analyses. *p*-values with a significance value of 0.05 and Cohen´s d effect size are reported. The individual FC values were FWE-corrected, after including age and sex as regressors. Differences in global ImCoh **A** and global wPLI **B** for five frequency bands.

Power and Functional connectivity – vertex-based and network-based analyses

After source reconstruction, the whole sample with DD was compared to matched controls at the vertex-level. The Desikan-Killiany atlas[42] was used for labeling of significant vertices. Figure 3 illustrates statistically significant differences in power and FC between groups.

Children with DD demonstrated left hemisphere differences in multiple measures compared to controls. Children with DD had lower power values in delta and theta frequency bands in the left parieto-occipital regions. FC analyses indicated lower FC ImCoh and wPLI values in theta band and greater ImCoh values in alpha band, both findings predominantly in the left hemisphere. Lower theta ImCoh and wPLI values compared to controls included vertices within the left middle frontal gyrus, precentral gyrus, temporal pole, middle and superior temporal gyrus, precuneus, supramarginal and angular gyrus. In the right hemisphere, lower theta FC was seen within the right precuneus, right cuneus, paracentral, and right occipito-temporal gyri. Greater alpha ImCoh values compared to controls were found for left fronto-temporo-parietal vertices, and to a lesser extent for right fronto-temporal vertices, and their midline structures. These midline structures included the left supramarginal gyrus, middle frontal gyrus, precentral gyrus, pars triangularis and opercularis, superior temporal gyrus, and temporal pole. **Supplementary Table 1** summarizes the results of all vertices with significant power and FC differences after Desikan-Killiany atlas labelling.

In addition, after data resampling and new permutational analyses between the whole sample with DD and matched controls was performed, but this time using the 7-network RSN Yeo atlas[43] for labelling. Table 3 summarizes significant power and FC differences in classical RSNs.

Table 3
Significant power or FC differences in RSNs, after analysis with the 7-Network Yeo atlas.

	Contrast	Dyslexia < Control						Dyslexia > Control		
	Frequency band	Delta			Theta			Alpha		
Metric	RSNs	*p*FWE	log10(*p*FWE)	Cohen´s *d*	*p*FWE	log10(*p*FWE)	Cohen´s *d*	*p*FWE	log10(*p*FWE)	Cohen´s *d*
Power	Left Dorsal Attention	0.05	1.32	0.57	–	–	–	–	–	–
	Left Visual	0.02	1.68	0.67	0.02	1.78	0.69	–	–	–
	Right Visual	–	–	–	0.05	1.31	0.57	–	–	–
ImCoh	Left Dorsal Attention	–	–	–	0.01	2.13	0.77	–	–	–
	Left Frontoparietal	–	–	–	0.01	1.91	0.72	–	–	–
	Left Default Mode	–	–	–	0.01	2.17	0.78	–	–	–
	Left Somatomotor	–	–	–	0.01	1.96	0.73	0.04	1.38	0.58
	Left Ventral Attention	–	–	–	0.03	1.58	0.64	0.03	1.46	0.61
	Right Dorsal Attention	–	–	–	0.04	1.36	0.58	–	–	–
	Right Default Mode	–	–	–	–	–	–	0.03	1.49	0.62
	Right Visual	–	–	–	0.02	1.82	0.70	–	–	–
	Right Limbic	–	–	–	–	–	–	0.03	1.58	0.64
wPLI	Left Dorsal Attention	–	–	–	0.01	2.14	0.77	–	–	–
	Left Frontoparietal	–	–	–	0.03	1.57	0.64	–	–	–
	Left Default Mode	–	–	–	0.03	1.47	0.61	–	–	–
	Right Visual	–	–	–	0.02	1.73	0.68	–	–	–
Note: -log10(pFWE) values have a significance threshold of 1.3 (p ≤ 0.05)(in a scale of 1.3 to 3).										

Participants with DD exhibited lower power in delta in the left dorsal attention and visual networks, and significantly lower values in theta and significantly lower values in theta for the left dorsal and ventral attention, fronto-parietal, and DMN, as well for the right dorsal attention, DMN, visual, and limbic networks. Greater theta power was observed in the bilateral visual networks. Finally, the ImCoh analysis demonstrated a significantly greater FC in alpha for the left somatomotor and ventral attention networks, but also the right DMN and limbic network. **Supplementary Fig. 1** illustrates these source reconstructed significant power and FC differences in RSNs.

Stratified vertex-based comparisons between 1st -4th and 5th -8th school grades groups and age matched controls found a decrease in power in the left parieto-occipital vertices in delta and theta in children with DD from 1st -4th grades. Similarly, theta ImCoh and wPLI were significantly decreased for 1st -4th graders but significantly increased alpha ImCoh for 5th -8th graders with DD for widespread bilateral regions. Figure 4 illustrates results from these comparisons.

Concerning the whole group of DD and controls, **Supplementary Fig. 2** displays the vertex-based effect of age, as it was included as a regressor in PALM. Power had the most significant negative effects in the delta and theta bands, spanning all vertices. These *p*FWE values were lower but still significant for the negative age effects over power in alpha and beta 2 bands in bilateral fronto-temporo-parietal vertices. Both ImCoh and wPLI indicated significant positive effects of age over alpha for bilateral temporo-occipital vertices. Finally, positive effects of age in beta 1–2 bands for multiple bilateral fronto-temporo-parietal vertices were restricted to ImCoh, with the highest values in left superior temporal and midline temporal vertices.

Correlations between power or FC, and cognitive performance

At a global level, a significant, moderate, negative Spearman correlation between power in theta band and text segments reading was found (p = 0.027, *rho*=-0.402, n = 37). Inspection of the partial rank correlation suggested that controlling for age had a slight but non-significant effect on the strength of correlation (p = 0.166, *rho*=-0.293) (Fig. 5A). Additionally, a non-significant, moderate, positive Spearman correlation between power in theta band and spelling was observed (p = 0.052, *rho* = 0.280, n = 63), but the corresponding partial rank correlation was significant (p = 0.045, *rho* = 0.289) (Fig. 5B). At a regional level, significant and moderate Spearman correlations were negative between power/ImCoh in theta band and text segments/words reading, but positive between power in theta band and spelling (Table 4). A floor effect was observed in z-scores of words reading, pseudowords reading, and text segments reading, but not for spelling (Fig. 5 and **Supplementary Fig. 3**). No other significant correlations were found for power, FC, and the rest of the cognitive subtests.

Table 4
Significant correlations between in-mask regional averages in theta band and performance in reading and spelling subtests.

					Spearman		Partial rank	
Metric	**Subtest**	**FDR-corrected regions**	**Regions (Desikan-Killiany labels)**	**Vertices**	***p*(FDR)**	**Rho**	***p*(FDR)**	**Rho**
Power	Text segments reading	5	Left occipital pole	12	**0.045**	-0.355	0.217	-0.243
			Left middle occipital gyrus	13	**0.045**	-0.344	0.217	-0.232
			Left calcarine sulcus	17	**0.045**	-0.371	0.217	-0.255
			Left intraparietal and transverse occipital sulci	16	**0.027**	-0.446	0.167	-0.356
	Spelling	5	Left occipital pole	12	**0.029**	0.323	**0.027**	0.331
			Left medial/lingual occipitotemporal gyrus	15	**0.029**	0.296	**0.027**	0.302
			Left middle occipital gyrus	13	**0.029**	0.285	**0.027**	0.291
			Left calcarine sulcus	17	**0.029**	0.294	**0.027**	0.300
			Left intraparietal and transverse occipital sulci	16	**0.049**	0.248	**0.041**	0.260
ImCoh	Words reading	8	Right paracentral gyrus and sulcus	11	**0.049**	-0.323	0.061	-0.328
			Right precuneus	11	**0.049**	-0.321	0.061	-0.314

Note: FDR applied with a rate of 0.05. The results belong to the Dyslexia < Controls contrast.

Discussion

We evaluated power and phase-based FC using routine clinical resting-state EEG data in children with DD compared to controls to test for resting-state power and FC differences on global and local levels.

We have confirmed our hypothesis that there are differences in regional power between children with DD and controls. Specifically, we observed differences in the delta and theta bands at both global and local levels, with a particular emphasis on the parieto-occipital regions of the left hemisphere. These regions correspond to the left dorsal attention and visual RSNs. While previous sensor-level studies did not detect power changes in children with DD[33,34,75], a study that used LORETA source-reconstruction found lower alpha power within temporo-parieto-occipital sources[35]. Since sensor-level analyses can be susceptible to volume conduction and allow indirect anatomical localization[76], our source reconstructed results offer improved anatomical precision of brain sources showing power and FC differences in children with DD. We found significantly lower delta-theta band power in the left parieto-occipital regions, which can be interpreted as a sign of parieto-occipital hypoactivation as demonstrated by previous fMRI studies of DD[14–16, 77]. These findings are potentially consistent with the magnocellular theory of dyslexia, which proposes abnormal interactions between magnocellular and parvocellular cells underlying reading-related visual processing deficits, although this theory still requires confirmation[25]. In this direction, motion perception and VWFA processing deficits have been found previously in children with DD[26,27,78], and others have proposed the existence of temporal sampling deficits in the visual system in addition to the temporal sampling deficits for speech/auditory stimuli[28,29].

We confirmed our hypothesis that there are resting-state connectivity changes between children with DD and controls. Both ImCoh and wPLI indicate significantly lower FC in theta for widespread left hemisphere vertices and numerous right parieto-occipital vertices. The ImCoh metric showed significantly higher FC predominantly within left fronto-temporo-parietal vertices, but also in multiple right fronto-temporal vertices. These differences correspond to RSNs in both hemispheres, namely, the left dorsal attention, frontoparietal, DMN, somatomotor, and ventral attention, but also the right dorsal attention, DMN, and visual RSNs. The reliability of our results is supported by the fact that two phase-based connectivity metrics take different properties of the EEG signal into account[55], and that previous resting-state EEG studies already found differences using the phase lag index (PLI)[33,34]. Therefore, our data suggests that children with DD show significant differences in FC not restricted to the reading and language networks, but extended to other RSNs. Although the Yeo atlas[43] does not provide annotations for the language network, it is an atlas derived from rs-fMRI data and there is evidence from whole-brain rs-fMRI studies of children with DD indicating that their reading-related regions are distributed among different RSNs[30,31]. Furthermore, fMRI investigations demonstrated decreased FC between the left VWFA and inferior frontal gyrus, and increased FC to the right hemisphere in participants with DD[31,78,79]. Other rs-fMRI studies have found abnormal FC patterns between multiple regions of the language network and the DMN in children with DD, corresponding to multiple regions where we observed greater alpha or lower theta FC[14,20,32]. In addition, our results of reduced theta FC in widespread left hemisphere regions are compatible with those from resting-state EEG and MEG studies that pointed to reduced network integration and impaired dynamic information flow in regions recruited during visual word processing and letter-speech sound associations[35,36,80], as well as reduced temporal correlations in left temporo-parietal sensors in beta band (local efficiency)[37–39]. Both findings of increased alpha FC and decreased theta FC within left frontal to occipital regions suggest that abnormal power and FC patterns may underlie temporal sampling deficits for separated or integrated phonological and visual processing[5,22,24,29,81]. To this extent, they may also underlie the atypical phase synchronization patterns during phonological and speech processing[18,21]. At the clinical level, the atypical FC in multiple RSNs can be a neurophysiological constraint that may partially explain their phonological processing and reading speed deficits[1, 82–85] involving right hemisphere regions as a potential compensatory mechanism to the constraints at the phonological, sublexical, and lexical linguistic processing levels[1,16,17,77,86].

The age-stratified comparisons revealed FC differences between the 1st -4th and 5th -8th school grade subgroups, which can be explained by previous research on normal developmental trajectories of EEG power and FC. Specifically, delta and theta power decrease throughout childhood and adolescence, while alpha to beta power increases[87–89]. Moreover, coherency measures increase globally between 8 and 12 years of age in all frequency bands except theta[90,91], whereas wPLI increases in theta, alpha, and beta bands, in fronto-parietal, frontal-occipital, and frontal-postcentral regions, respectively[88]. The lower wPLI in the theta band observed in our 1st -4th graders is consistent with the finding of logarithmically increasing wPLI values in the left parietal cortex in the theta band across normal development[88], which may be a neurodevelopmental marker of difficulties in writing skills during early literacy acquisition, as this region is involved in meaning processing and writing[1,88,92,93]. Moreover, the increased wPLI in alpha in the left prefrontal regions of 5th -8th graders with DD may reflect increased demands for cognitive control, possibly as a coping strategy in early adolescence[88]. However, changes in power and FC across development with and without DD are matters outside the scope of the current cross-sectional design. Future investigations with larger samples and a wider age range are needed to test these hypotheses.

Lastly, we found variable correlations between power and FC and cognitive metrics. Increased theta power within the left parieto-occipital regions was correlated with increased spelling scores, whereas a decrease in theta power was associated with improved reading scores. We suggest that the difference in correlation is due to a clear floor effect in the reading scores (Fig. 5A). This makes the spelling data the most robust and useful to interpretation (Fig. 5B). It is emphasized that 20 children with DD assessed with SLRT-II or ZLT-II were unable to read more items than the equivalent to the first percentile rank and, as a consequence, the group showed particularly low z-scores and high standard deviations in reading subtests (Table 2), pointing to a tendency to severe dyslexia in our sample. Therefore, after controlling for age, a significant partial rank correlation between lower theta power in five left parieto-occipital regions and poor spelling performance (Table 4) can be explained by a decreased efficiency in sublexical processing in children with DD, i.e. the ability to use grapheme-phoneme correspondence rules either in the reading or spelling direction[94,95]. Furthermore, it is possible that decreased power in the left parieto-occipital regions relates to reduced long-range communication with other language-related regions, a finding of the aforementioned resting-state EEG/MEG studies of DD[33,34,39]. Finally, this finding may be related to parieto-occipital hypoactivation in fMRI[14–16, 77,96], disrupted FC between left parieto-occipital regions (including VWFA) and inferior frontal regions[32,79], and poorer visual letter-word recognition, meaning processing, and decreased reading time when children with DD are compared to controls[35,36,80].

Limitations and conclusion

Our study has limitations. First, the retrospective design limits clinical and neuropsychological information. Clinical EEG data was restricted to 19 channels, which impacts spatial resolution. However, there is evidence of the feasibility of low-density EEG studies for IED source localization[97,98], and the feasibility of FC and power analyses from source reconstruction of low-density EEG[41]. Indeed, the ability to use low resolution to identify differences could be a strength if these RSN features become a supportive diagnostic marker for DD. The duration of analyzed EEG was also limited. Ideally, 3–6 minutes of resting-state data should be used[52,99], but we could analyze 50 seconds of clean data. Other groups have used data lengths from seconds to 1 minute, providing meaningful findings[100–103].

In the neuropsychological data, many participants did not have handedness documented and it was available for the DD group. To our knowledge, there is no evidence of differential effects of handedness over connectivity in DD. In fact, a significant correlation between reading improvement and fractional anisotropy measures in age- and handedness-matched children with DD was found in a longitudinal fMRI and diffusion tensor imaging (DTI) study[17]. Future prospective studies of DD might test if FC measures differ due to handedness and collect neuropsychological data from controls so a true comparison of cognitive abilities and RSNs can be assessed.

In summary, power and FC analyses applied to source reconstructed resting-state and clinical routine EEG confirmed significant differences in multiple left language-related regions but also pertaining to other RSNs. In addition, a significant correlation between power in left parieto-occipital regions and poor spelling performance in children with DD in 1st -4th school grades suggests that future investigations approach the development of spelling disorder in DD, also in relation to power and FC. Consequently, the current study supports an atypical functional organization in DD, supporting findings from previous resting-state EEG, rs-fMRI, and MEG studies. To our knowledge, this is the first study implementing source reconstruction for low-density EEG to test simultaneously power and FC differences of children with DD. We suggest these methods to continue studying the electroencephalographical signatures of DD and other neurodevelopmental disorders[30,44,104].

Abbreviations

ADD/ADHD
attention deficit with/without hyperactivity
DD
developmental dyslexia
DMN
default mode network
DTI
diffusion tensor imaging
EEG
electroencephalography
FC
functional connectivity
FDR
false discovery rate
FFT
Fast Fourier Transformation
fMRI
functional resonance imaging
FRI
fluid reasoning index
FSIQ
full-scale intellectual quotient
FWE
Family wise error
GLM
general linear model
HAWIK
Hamburg-Wechsler-Intelligenztest für Kinder
HSP
Hamburger Schreib-Probe

ICA
independent component analysis
IEDs
interictal epileptiform discharges
ImCoh
imaginary part of coherency
LORETA
low-resolution brain electromagnetic tomography
MEG
magnetoencephalography
MST
minimum spanning tree
PALM
Permutation Analysis of Linear Models
PLI
phase lag index
PRs
percentage ranks
PSI
processing speed index
rs-fMRI
resting-state functional magnetic resonance imaging
RSNs
resting-state networks
SD
Standard deviation
SLRT
Salzburger Lesetest
TFCE
threshold-free cluster enhancement
TOWRE
Test of Word Reading Efficiency
VCI
verbal comprehension index
VSI
visual-spatial index
VWFA
visual word form area
WISC
Wechsler Intelligence Scale for Children
WMI
working memory index
wPLI
weighted phase lag index
WRT
Weingartener Grundwortschatz Rechtschreib-Tests
ZLT
Zürcher Lesetest.

Declarations

Ethics approval: This work was approved by the Ethics Committee of the University Medical Center of Göttingen (reference number 05.12.19).

Consent for publication: Not applicable.

Availability of data and materials: The datasets used and analyzed during the current study are available from the corresponding author on reasonable request.

Competing interests: N.F. received honoraria from Arvelle, Jazz Pharma, Bial, Eisai, and EGI-Phillips, all unrelated to the current work. We acknowledge support by the Open Access Publication Funds of the Göttingen University. All other authors report no disclosures.

Funding: DG was funded by the German Academic Exchange Service (DAAD), which had no role during the research process.

Authors` contributions: DG, design and conceptualization of the study, acquisition of data, analysis of the data, drafting and revision of the manuscript. **SDWS,** analysis of the data, drafting and revision of the manuscript. **DV:** analysis of the data, revision of the manuscript. **CS:** analysis of the data, revision of the manuscript. **KB:** conceptualization of the study, revision of the manuscript. **SS:** analysis of the data, revision of the manuscript. **NN:** analysis of the data, revision of the manuscript. **NF:** design and conceptualization of the study, analysis of the data, revision of the manuscript, project supervision.

Acknowledgments: Not applicable.

References

1. Kearns DM, Hancock R, Hoeft F, Pugh KR, Frost SJ. The Neurobiology of Dyslexia. Teach Except Child. 2019;51(3):175–88. 10.1177/0040059918820051.
2. Skeide MA, Evans TM, Mei EZ, Abrams DA, Menon V. Neural signatures of co-occurring reading and mathematical difficulties. Dev Sci. 2018;21(6):1–11. 10.1111/desc.12680.
3. American Psychiatric Association. Diagnostic and Statistical Manual of Mental Disorders. American Psychiatric Association; 2013. 10.1176/appi.books.9780890425596.
4. Lyon GR, Sl B, Catts H, et al. A Definition of Dyslexia. Ann Dyslexia. 2003;53(1):1–14. http://www.hku.hk/linguist/cou/adv/ling6022/articles/lyon2003.pdf.
5. Hancock R, Pugh KR, Hoeft F. Neural Noise Hypothesis of Developmental Dyslexia. Trends Cogn Sci. 2017;21(6):434–48. 10.1016/j.tics.2017.03.008.
6. Wagner RK, Zirps FA, Edwards AA, et al. The Prevalence of Dyslexia: A New Approach to Its Estimation. J Learn Disabil. 2020;53(5):354–65. 10.1177/0022219420920377.
7. Landerl K, Moll K. Comorbidity of learning disorders: Prevalence and familial transmission. J Child Psychol Psychiatry Allied Discip. 2010;51(3):287–94. 10.1111/j.1469-7610.2009.02164.x.
8. Moll K, Kunze S, Neuhoff N, Bruder J, Schulte-Körne G. Specific learning disorder: Prevalence and gender differences. PLoS ONE. 2014;9(7). 10.1371/journal.pone.0103537.
9. D'mello AM, Gabrieli JDE. Cognitive neuroscience of dyslexia. Lang Speech Hear Serv Sch. 2018;49(4):798–809. 10.1044/2018_LSHSS-DYSLC-18-0020.
10. Visser L, Kalmar J, Linkersdörfer J, et al. Comorbidities Between Specific Learning Disorders and Psychopathology in Elementary School Children in Germany. Front Psychiatry. 2020;11(April):1–12. 10.3389/fpsyt.2020.00292.
11. Pugh KR, Einar Mencl W, Jenner AR, et al. Functional neuroimaging studies of reading and reading disability (developmental dyslexia). Ment Retard Dev Disabil Res Rev. 2000;6(3):207–13. 10.1002/1098-2779(2000)6:3<207::AID-MRDD8>3.0.CO;2-P.
12. Raschle NM, Zuk J, Gaab N. Functional characteristics of developmental dyslexia in left-hemispheric posterior brain regions predate reading onset. Proc Natl Acad Sci U S A. 2012;109(6):2156–61. 10.1073/pnas.1107721109.
13. Richlan F, Kronbichler M, Wimmer H. Functional abnormalities in the dyslexic brain: A quantitative meta-analysis of neuroimaging studies. Hum Brain Mapp. 2009;30(10):3299–308. 10.1002/hbm.20752.
14. Richlan F, Sturm D, Schurz M, Kronbichler M, Ladurner G, Wimmer H. A common left occipito-temporal dysfunction in developmental dyslexia and acquired letter-by-letter reading? PLoS ONE. 2010;5(8):9–11. 10.1371/journal.pone.0012073.
15. Richlan F, Kronbichler M, Wimmer H. Meta-analyzing brain dysfunctions in dyslexic children and adults. NeuroImage. 2011;56(3):1735–42. 10.1016/j.neuroimage.2011.02.040.
16. Martin A, Kronbichler M, Richlan F. Dyslexic brain activation abnormalities in deep and shallow orthographies: A meta-analysis of 28 functional neuroimaging studies. Hum Brain Mapp. 2016;37(7):2676–99. 10.1002/hbm.23202.
17. Hoeft F, McCandliss BD, Black JM, et al. Neural systems predicting long-term outcome in dyslexia. Proc Natl Acad Sci U S A. 2011;108(1):361–6. 10.1073/pnas.1008950108.

18. De Vos A, Vanvooren S, Vanderauwera J, Ghesquière P, Wouters J. Atypical neural synchronization to speech envelope modulations in dyslexia. Brain Lang. 2017;164:106–17. 10.1016/j.bandl.2016.10.002.
19. Molinaro N, Lizarazu M, Lallier M, Bourguignon M, Carreiras M. Out-of-synchrony speech entrainment in developmental dyslexia. Hum Brain Mapp. 2016;37(8):2767–83. 10.1002/hbm.23206.
20. Kuhl U, Neef NE, Kraft I, et al. The emergence of dyslexia in the developing brain. NeuroImage. 2020;211(February). 10.1016/j.neuroimage.2020.116633.
21. Mandke K, Flanagan S, Macfarlane A, et al. Neural sampling of the speech signal at different timescales by children with dyslexia. NeuroImage. 2022;253(January):119077. 10.1016/j.neuroimage.2022.119077.
22. Goswami U. A neural oscillations perspective on phonological development and phonological processing in developmental dyslexia. Lang Linguist Compass. 2019;13(5):1–21. 10.1111/lnc3.12328.
23. Keshavarzi M, Mandke K, Macfarlane A, et al. Decoding of speech information using EEG in children with dyslexia: Less accurate low-frequency representations of speech, not "Noisy" representations. Brain Lang. 2022;235(March):105198. 10.1016/j.bandl.2022.105198.
24. Goswami U. A temporal sampling framework for developmental dyslexia. Trends Cogn Sci. 2011;15(1):3–10. 10.1016/j.tics.2010.10.001.
25. Stein J. The current status of the magnocellular theory of developmental dyslexia. Neuropsychologia. 2019;130(September 2017):66–77. 10.1016/j.neuropsychologia.2018.03.022.
26. Gori S, Cecchini P, Bigoni A, Molteni M, Facoetti A. Magnocellular-dorsal pathway and sub-lexical route in developmental dyslexia. Front Hum Neurosci. 2014;8(JUNE):1–11. 10.3389/fnhum.2014.00460.
27. Gori S, Seitz AR, Ronconi L, Franceschini S, Facoetti A. Multiple Causal Links between Magnocellular-Dorsal Pathway Deficit and Developmental Dyslexia. Cereb Cortex. 2016;26(11):4356–69. 10.1093/cercor/bhv206.
28. Vidyasagar TR. Reading into neuronal oscillations in the visual system: Implications for developmental dyslexia. Front Hum Neurosci. 2013;7(NOV):1–10. 10.3389/fnhum.2013.00811.
29. Archer K, Pammer K, Vidyasagar TR. A Temporal Sampling Basis for Visual Processing in Developmental Dyslexia. Front Hum Neurosci. 2020;14(July):1–24. 10.3389/fnhum.2020.00213.
30. Bailey SK, Aboud KS, Nguyen TQ, Cutting LE. Applying a network framework to the neurobiology of reading and dyslexia. J Neurodev Disord. 2018;10(1):1–9. 10.1186/s11689-018-9251-z.
31. Finn ES, Shen X, Holahan JM, et al. Disruption of functional networks in dyslexia: A whole-brain, data-driven analysis of connectivity. Biol Psychiatry. 2014;76(5):397–404. 10.1016/j.biopsych.2013.08.031.
32. Schurz M, Wimmer H, Richlan F, Ludersdorfer P, Klackl J, Kronbichler M. Resting-state and task-based functional brain connectivity in developmental dyslexia. Cereb Cortex. 2015;25(10):3502–14. 10.1093/cercor/bhu184.
33. Fraga González G, Van der Molen MJW, Žarić G, et al. Graph analysis of EEG resting state functional networks in dyslexic readers. Clin Neurophysiol. 2016;127(9):3165–75. 10.1016/j.clinph.2016.06.023.
34. Xue H, Wang Z, Tan Y, et al. Resting-state EEG reveals global network deficiency in dyslexic children. Neuropsychologia. 2020;138(June 2019):107343. 10.1016/j.neuropsychologia.2020.107343.
35. Babiloni C, Stella G, Buffo P, et al. Cortical sources of resting state EEG rhythms are abnormal in dyslexic children. Clin Neurophysiol. 2012;123(12):2384–91. 10.1016/j.clinph.2012.05.002.
36. Bosch-Bayard J, Girini K, Biscay RJ, Valdes-Sosa P, Evans AC, Chiarenza GA. Resting EEG effective connectivity at the sources in developmental dysphonetic dyslexia. Differences with non-specific reading delay. Int J Psychophysiol. 2020;153(February):135–47. 10.1016/j.ijpsycho.2020.04.021.
37. Dimitriadis SI, Laskaris NA, Simos PG, Fletcher JM, Papanicolaou AC. Greater repertoire and temporal variability of cross-frequency coupling (CFC) modes in resting-state neuromagnetic recordings among children with reading difficulties. Front Hum Neurosci. 2016;10(APR2016):1–17. 10.3389/fnhum.2016.00163.
38. Dimitriadis SI, Laskaris NA, Simos PG, et al. Altered temporal correlations in resting-state connectivity fluctuations in children with reading difficulties detected via MEG. NeuroImage. 2013;83:307–17. 10.1016/j.neuroimage.2013.06.036.
39. Dimitriadis SI, Simos PG, Fletcher J, Papanicolaou AC. Aberrant resting-state functional brain networks in dyslexia: Symbolic mutual information analysis of neuromagnetic signals. Int J Psychophysiol. 2018;126(February):20–9. 10.1016/j.ijpsycho.2018.02.008.
40. Gross J, Kujala J, Hämäläinen M, Timmermann L, Schnitzler A, Salmelin R. Dynamic imaging of coherent sources: Studying neural interactions in the human brain. Proc Natl Acad Sci U S A. 2001;98(2):694–9. 10.1073/pnas.98.2.694.
41. Nguyen-Danse DA, Singaravelu S, Chauvigné LAS, Mottaz A, Allaman L, Guggisberg AG. Feasibility of Reconstructing Source Functional Connectivity with Low-Density EEG. Brain Topogr. 2021;34(6):709–19. 10.1007/s10548-021-00866-w.

42. Desikan RS, Ségonne F, Fischl B, et al. An automated labeling system for subdividing the human cerebral cortex on MRI scans into gyral based regions of interest. NeuroImage. 2006;31(3):968–80. 10.1016/j.neuroimage.2006.01.021.
43. Thomas Yeo BT, Krienen FM, Sepulcre J, et al. The organization of the human cerebral cortex estimated by intrinsic functional connectivity. J Neurophysiol. 2011;106(3):1125–65. 10.1152/jn.00338.2011.
44. Brimo K, Dinkler L, Gillberg C, Lichtenstein P, Lundström S, Åsberg Johnels J. The co-occurrence of neurodevelopmental problems in dyslexia. Dyslexia. 2021;27(3):277–93. 10.1002/dys.1681.
45. Germanò E, Gagliano A, Curatolo P. Comorbidity of ADHD and dyslexia. Dev Neuropsychol. 2010;35(5):475–93. 10.1080/87565641.2010.494748.
46. Margari L, Buttiglione M, Craig F, Cristella A, de Giambattista, Matera E, Operto F, Simone M. Neuropsychopathological comorbidities in learning disorders. PLoS ONE. 2014;9(7):1–6. 10.1371/journal.pone.0103537.
47. Oostenveld R, Fries P, Maris E, Schoffelen JM, FieldTrip. Open source software for advanced analysis of MEG, EEG, and invasive electrophysiological data. *Comput Intell Neurosci*. 2011;2011. doi:10.1155/2011/156869.
48. Berry R, Quan S, Abreu A. *The AASM Manual for the Scoring of Sleep and Associated Events: Rules, Terminology and Technical Specifications.* Version 2. American Academy of Sleep Medicine, Darien.; 2020. https://aasm.org/clinical-resources/scoring-manual/.
49. Kreilkamp BAK, Martin P, Bender B, et al. Big Field of View MRI T1w and FLAIR Template - NMRI225. Sci Data. 2022;1–8. 10.1038/s41597-023-02087-1.
50. Fischl B, FreeSurfer.. NeuroImage. 2012;62(2):774–81. 10.1016/j.neuroimage.2012.01.021.
51. Saad ZS, Reynolds RC, Suma. NeuroImage. 2012;62(2):768–73. 10.1016/j.neuroimage.2011.09.016.
52. Marquetand J, Vannoni S, Carboni M, et al. Reliability of Magnetoencephalography and High-Density Electroencephalography Resting-State Functional Connectivity Metrics. Brain Connect. 2019;9(7):539–53. 10.1089/brain.2019.0662.
53. Fraga González G, Smit DJA, van der Molen MJW, et al. EEG Resting State Functional Connectivity in Adult Dyslexics Using Phase Lag Index and Graph Analysis. Front Hum Neurosci. 2018;12(August):1–12. 10.3389/fnhum.2018.00341.
54. Nolte G, Bai O, Wheaton L, Mari Z, Vorbach S, Hallett M. Identifying true brain interaction from EEG data using the imaginary part of coherency. Clin Neurophysiol. 2004;115(10):2292–307. 10.1016/j.clinph.2004.04.029.
55. Vinck M, Oostenveld R, Van Wingerden M, Battaglia F, Pennartz CMA. An improved index of phase-synchronization for electrophysiological data in the presence of volume-conduction, noise and sample-size bias. NeuroImage. 2011;55(4):1548–65. 10.1016/j.neuroimage.2011.01.055.
56. Bowyer SM. Coherence a measure of the brain networks: past and present. Neuropsychiatr Electrophysiol. 2016;2(1):1–12. 10.1186/s40810-015-0015-7.
57. Yoshinaga K, Matsuhashi M, Mima T, et al. Comparison of Phase Synchronization Measures for Identifying Stimulus-Induced Functional Connectivity in Human Magnetoencephalographic and Simulated Data. Front Neurosci. 2020;14(June). 10.3389/fnins.2020.00648.
58. Li Hegner Y, Marquetand J, Elshahabi A, et al. Increased Functional MEG Connectivity as a Hallmark of MRI-Negative Focal and Generalized Epilepsy. Brain Topogr. 2018;31(5):863–74. 10.1007/s10548-018-0649-4.
59. Elshahabi A, Klamer S, Sahib AK, Lerche H, Braun C, Focke NK. Magnetoencephalography reveals a widespread increase in network connectivity in idiopathic/genetic generalized epilepsy. PLoS ONE. 2015;10(9):1–16. 10.1371/journal.pone.0138119.
60. Elisevich K, Shukla N, Moran JE, et al. An assessment of MEG coherence imaging in the study of temporal lobe epilepsy. Epilepsia. 2011;52(6):1110–9. 10.1111/j.1528-1167.2011.02990.x.
61. Englot DJ, Hinkley LB, Kort NS, et al. Global and regional functional connectivity maps of neural oscillations in focal epilepsy. Brain. 2015;138(8):2249–62. 10.1093/brain/awv130.
62. Choi HS, Chung YG, Choi SA, et al. Electroencephalographic resting-state functional connectivity of benign epilepsy with centrotemporal spikes. J Clin Neurol. 2019;15(2):211–20. 10.3988/jcn.2019.15.2.211.
63. Stier C, Elshahabi A, Li Hegner Y, et al. Heritability of Magnetoencephalography Phenotypes Among Patients With Genetic Generalized Epilepsy and Their Siblings. Neurology. 2021;97(2):e166–77. 10.1212/WNL.0000000000012144.
64. Martire DJ, Wong S, Workewych A, et al. Temporal-plus epilepsy in children: A connectomic analysis in magnetoencephalography. Epilepsia. 2020;61(8):1691–700. 10.1111/epi.16591.
65. Smith SM, Nichols TE. Threshold-free cluster enhancement: Addressing problems of smoothing, threshold dependence and localisation in cluster inference. NeuroImage. 2009;44(1):83–98. 10.1016/j.neuroimage.2008.03.061.
66. Torgesen JK, Wagner RK, Rashotte CA. Test Review: Test of Word Reading Efficiency–Second Edition (TOWRE-2) by, Torgesen JK, Wagner RK, Rashotte CA. *Can J Sch Psychol*. 2015;30(4):320–326. doi:10.1177/0829573515594334.

67. McCrimmon AW, Climie EA. Test Review: Test of Written Language—Fourth Edition. J Psychoeduc Assess. 2011;29(6):592–6. 10.1177/0734282911406646.
68. Larsen SC, Hammill DD, Moats LC. Test of Written Spelling, Fourth Edition, Test Review. J Psychoeduc Assess. 2005;23(1):189–95.
69. Iverson GL. Z Scores. In Kreutzer, JS, DeLuca, J, Caplan, B, editors. *Encyclopedia of Clinical Neuropsychology*. 2011. doi:10.1007/978-0-387-79948-3.
70. May P. *HSP 1–9 Diagnose Orthografischer Kompetenz. Zur Erfassung Der Grundlegenden Rechtschreibstrategien Mit Der Hamburger Schreibprobe*. (6, aktual. Hamburg: Verlag für Pädagogische Medien VPM; 2002.
71. Petermann F, Daseking M, Linder M, Grissemann H, Weid T. Zürcher Lesetest-II: ZLT-II; Weiterentwicklung DesZürcher Lesetests (ZLT). Bern: Huber; 2013.
72. Moll K, Landerl K. SLRT-II: Lese-Und Rechtschreibtest; Weiterentwicklung Des Salzburger Lese-Und Rechtschreibtests. Bern: Huber; 2010.
73. Petermann F, Petermann U. HAWIK-IV: Hamburg-Wechsler-Intelligenztest Für Kinder-IV; Manual; Übersetzung UndAdaption Der WISC-IV von David Wechsler. Bern: Huber; 2010.
74. Benjamini Y, Hochberg Y. Controlling the False Discovery Rate: A Practical and Powerful Approach to Multiple Testing. J R Stat Soc Ser B. 1995;57(1):289–300. 10.1111/j.2517-6161.1995.tb02031.x.
75. Papagiannopoulou EA, Lagopoulos J. Resting state EEG hemispheric power asymmetry in children with dyslexia. Front Pediatr. 2016;4(FEB). 10.3389/fped.2016.00011.
76. Schaworonkow N, Nikulin VV. Is sensor space analysis good enough? Spatial patterns as a tool for assessing spatial mixing of EEG/MEG rhythms. NeuroImage. 2022;253(August 2021):119093. 10.1016/j.neuroimage.2022.119093.
77. Shaywitz BA, Shaywitz SE, Pugh KR, et al. Disruption of posterior brain systems for reading in children with developmental dyslexia. Biol Psychiatry. 2002;52(2):101–10. 10.1016/S0006-3223(02)01365-3.
78. Brem S, Maurer U, Kronbichler M, et al. Visual word form processing deficits driven by severity of reading impairments in children with developmental dyslexia. Sci Rep. 2020;10(1):1–14. 10.1038/s41598-020-75111-8.
79. van der Mark S, Klaver P, Bucher K, et al. The left occipitotemporal system in reading: Disruption of focal fMRI connectivity to left inferior frontal and inferior parietal language areas in children with dyslexia. NeuroImage. 2011;54(3):2426–36. 10.1016/j.neuroimage.2010.10.002.
80. Žarić G, Correia JM, Fraga González G, et al. Altered patterns of directed connectivity within the reading network of dyslexic children and their relation to reading dysfluency. Dev Cogn Neurosci. 2017;23:1–13. 10.1016/j.dcn.2016.11.003.
81. Giraud AL, Poeppel D. Cortical oscillations and speech processing: Emerging computational principles and operations. Nat Neurosci. 2012;15(4):511–7. 10.1038/nn.3063.
82. Peterson RL, Pennington BF. Developmental dyslexia: The Lancet. Lancet. 2012;379(9830):1997–2007. 10.1016/S0140-6736(12)60198-6.
83. Schulte-Körne G. Diagnostik und therapie der lese-rechtschreib-störung gerd schulte-körne. Dtsch Arztebl. 2010;107(41):717–27. 10.3238/arztebl.2010.0718.
84. Giraud AL, Poeppel D. Cortical oscillations and speech processing: Emerging computational principles and operations. Nat Neurosci. 2012;15(4):511–7. 10.1038/nn.3063.
85. Goswami U. Sensory theories of developmental dyslexia: Three challenges for research. Nat Rev Neurosci. 2015;16(1):43–54. 10.1038/nrn3836.
86. Paz-Alonso PM, Oliver M, Lerma-Usabiaga G, et al. Neural correlates of phonological, orthographic and semantic reading processing in dyslexia. NeuroImage Clin. 2018;20(August):433–47. 10.1016/j.nicl.2018.08.018.
87. Cellier D, Riddle J, Petersen I, Hwang K. The development of theta and alpha neural oscillations from ages 3 to 24 years. Dev Cogn Neurosci. 2021;50:100969. 10.1016/j.dcn.2021.100969.
88. Hunt BAE, Wong SM, Vandewouw MM, Brookes MJ, Dunkley BT, Taylor MJ. Spatial and spectral trajectories in typical neurodevelopment from childhood to middle age. Netw Neurosci. 2019;3(2):497–520. 10.1162/netn_a_00077.
89. Marek S, Tervo-Clemmens B, Klein N, Foran W, Ghuman AS, Luna B. Adolescent development of cortical oscillations: Power, phase, and support of cognitive maturation. PLoS Biol. 2018;16(11):1–29. 10.1371/JOURNAL.PBIO.2004188.
90. Barry RJ, Clarke AR, McCarthy R, Selikowitz M, Johnstone SJ, Rushby JA. Age and gender effects in EEG coherence: I. Developmental trends in normal children. Clin Neurophysiol. 2004;115(10):2252–8. 10.1016/j.clinph.2004.05.004.
91. Anderson AJ, Perone S. Developmental change in the resting state electroencephalogram: Insights into cognition and the brain. Brain Cogn. 2018;126(January):40–52. 10.1016/j.bandc.2018.08.001.
92. Palmis S, Velay JL, Habib M, et al. The handwriting brain in middle childhood. Dev Sci. 2021;24(2):1–17. 10.1111/desc.13046.

93. Brownsett SLE, Wise RJS. The contribution of the parietal lobes to speaking and writing. Cereb Cortex. 2010;20(3):517–23. 10.1093/cercor/bhp120.
94. Goswami U, Mead N, Fosker T, Huss M, Barnes L, Leong V. Impaired perception of syllable stress in children with dyslexia: A longitudinal study. J Mem Lang. 2013;69(1):1–17. 10.1016/j.jml.2013.03.001.
95. Gangl M, Moll K, Jones MW, Banfi C, Schulte-Körne G, Landerl K. Lexical Reading in Dysfluent Readers of German. Sci Stud Read. 2018;22(1):24–40. 10.1080/10888438.2017.1339709.
96. Pugh KR, Einar Mencl W, Shaywitz BA, et al. The angular gyrus in developmental dyslexia: Task-specific differences in functional connectivity within posterior cortex. NeuroImage. 1999;9(6 PART II):51–6.
97. Sharma P, Scherg M, Pinborg LH, et al. Ictal and interictal electric source imaging in pre-surgical evaluation: a prospective study. Eur J Neurol. 2018;25(9):1154–60. 10.1111/ene.13676.
98. Baroumand AG, van Mierlo P, Strobbe G, et al. Automated EEG source imaging: A retrospective, blinded clinical validation study. Clin Neurophysiol. 2018;129(11):2403–10. 10.1016/j.clinph.2018.09.015.
99. Rolle CE, Narayan M, Wu W, et al. Functional connectivity using high density EEG shows competitive reliability and agreement across test/retest sessions. J Neurosci Methods. 2022;367(November 2021):109424. 10.1016/j.jneumeth.2021.109424.
100. Demuru M, Fraschini M. EEG fingerprinting: Subject-specific signature based on the aperiodic component of power spectrum. Comput Biol Med. 2020;120(February):103748. 10.1016/j.compbiomed.2020.103748.
101. Chu CJ, Kramer MA, Pathmanathan J, et al. Emergence of stable functional networks in long-term human electroencephalography. J Neurosci. 2012;32(8):2703–13. 10.1523/JNEUROSCI.5669-11.2012.
102. Ahmadlou M, Adeli H. Functional community analysis of brain: A new approach for EEG-based investigation of the brain pathology. NeuroImage. 2011;58(2):401–8. 10.1016/j.neuroimage.2011.04.070.
103. Bosch-Bayard J, Biscay RJ, Fernandez T, et al. EEG effective connectivity during the first year of life mirrors brain synaptogenesis, myelination, and early right hemisphere predominance. NeuroImage. 2022;252(November 2021):119035. 10.1016/j.neuroimage.2022.119035.
104. Langer N, Benjamin C, Becker BLC, Gaab N. Comorbidity of reading disabilities and ADHD: Structural and functional brain characteristics. Hum Brain Mapp. 2019;40(9):2677–98. 10.1002/hbm.24552.

Figures

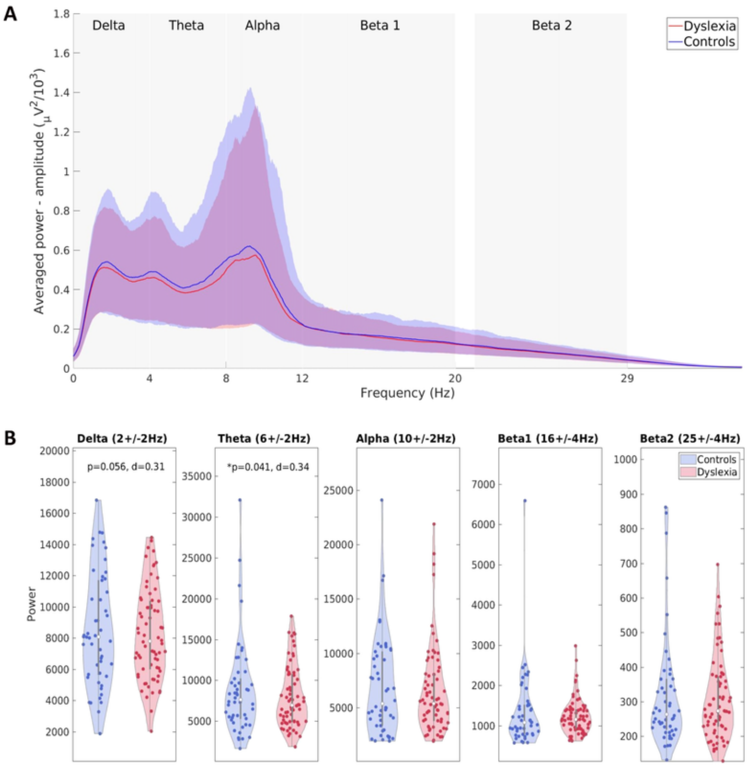

Figure 1

Absolute power spectral analysis. **A** Power spectra averaged across 19 scalp channels for the dyslexic and control groups, calculated at sensor-level. The shaded areas represent 95% confidence intervals. **B** Violin plots of differences in global power between children with DD and controls, after source-level analysis. The individual power values were FWE-corrected, after including age and sex as regressors.

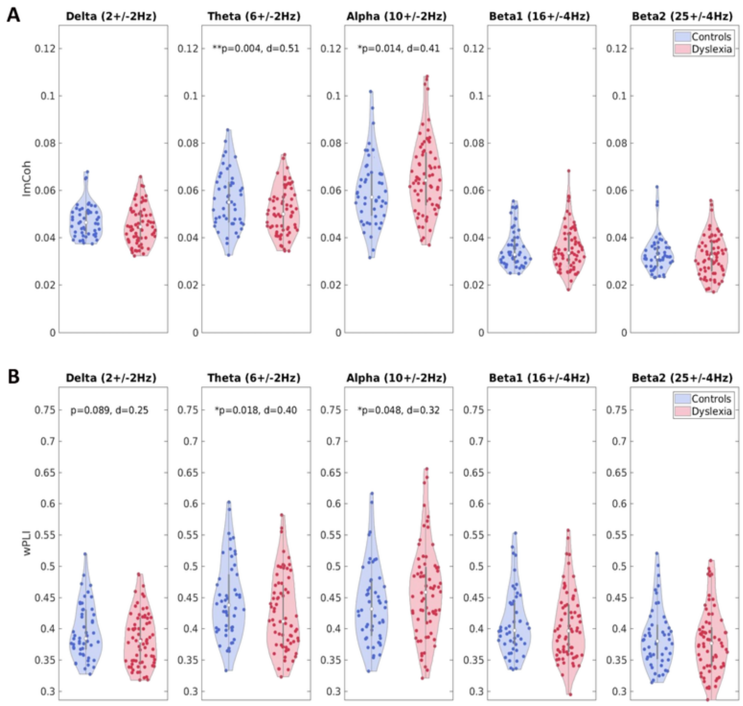

Figure 2

Violin plots of global FC metrics comparing children with DD and controls, after source-level analyses. p-values with a significance value of 0.05 and Cohen´s d effect size are reported. The individual FC values were FWE-corrected, after including age and sex as regressors. Differences in global ImCoh **A** and global wPLI **B** for five frequency bands.

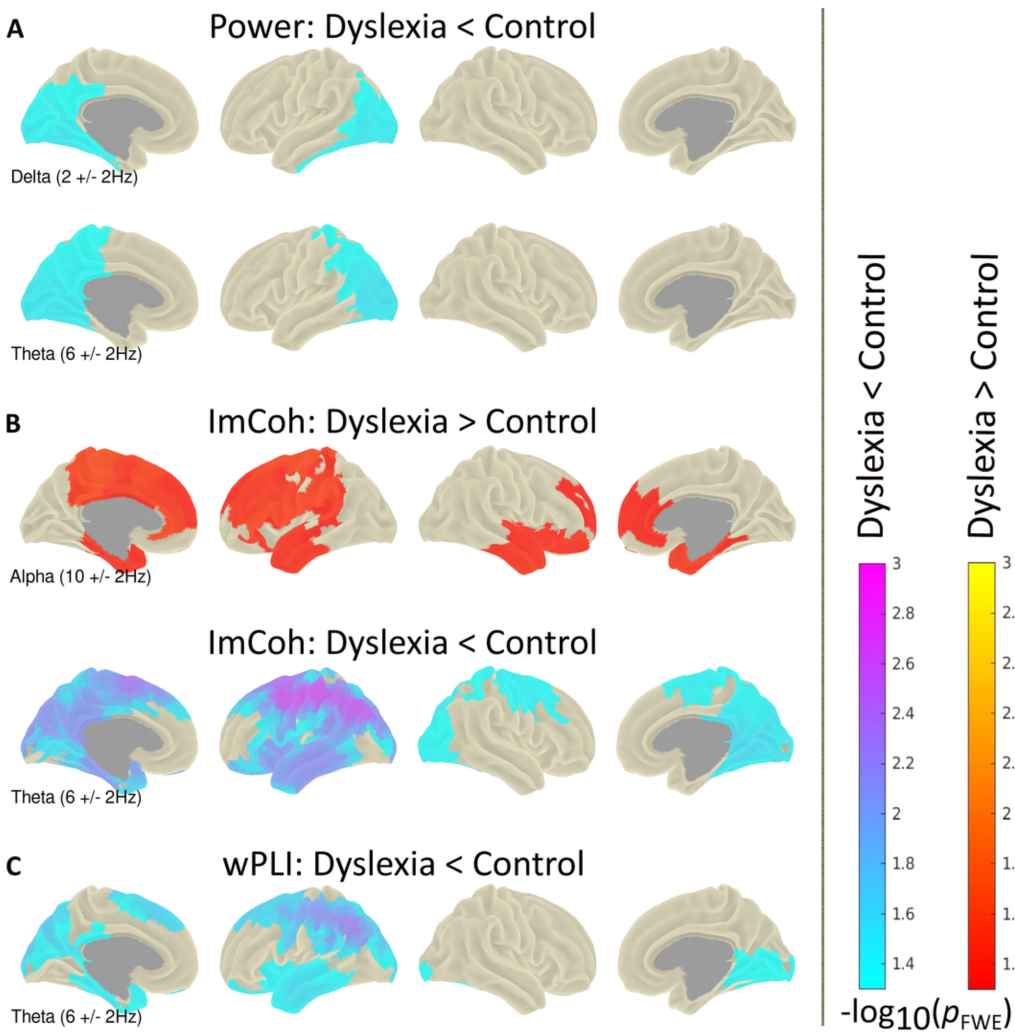

Figure 3

Vertices with significant differences in **A** power, **B** ImCoh, and **C** wPLI are exhibited. p-values were familywise error corrected (FWE) and are indicated as -$\log_{10}$(p-value), with a significance threshold of 1.3 ($p \leq 0.05$)(in a scale of 1.3 to 3).

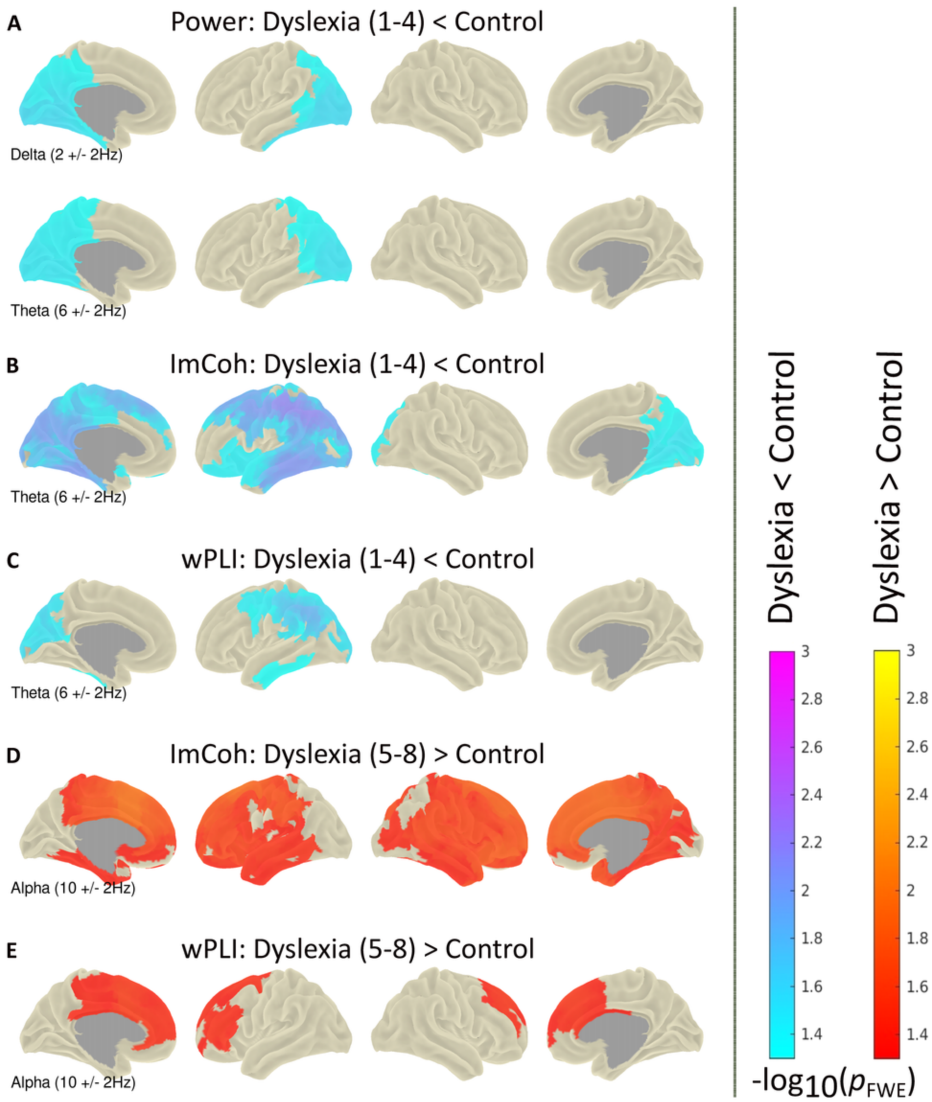

Figure 4

Vertices with significant differences between children with DD in different school grades and age matched controls. **A** power, **B** ImCoh, and **C** wPLI differences between DD in 1st-4th school grades (58 children) and controls (38 children). **D** ImCoh, and **E** wPLI differences between DD in 5th to 8th school grades (12 children) and controls (12 children). p-values were familywise error corrected (FWE) and are indicated as -log10$_p$, with a significance threshold of 1.3 ($p \leq 0.05$)(in a scale of 1.3-3). No significant power differences were found for 5th-8th school graders vs. matched controls.

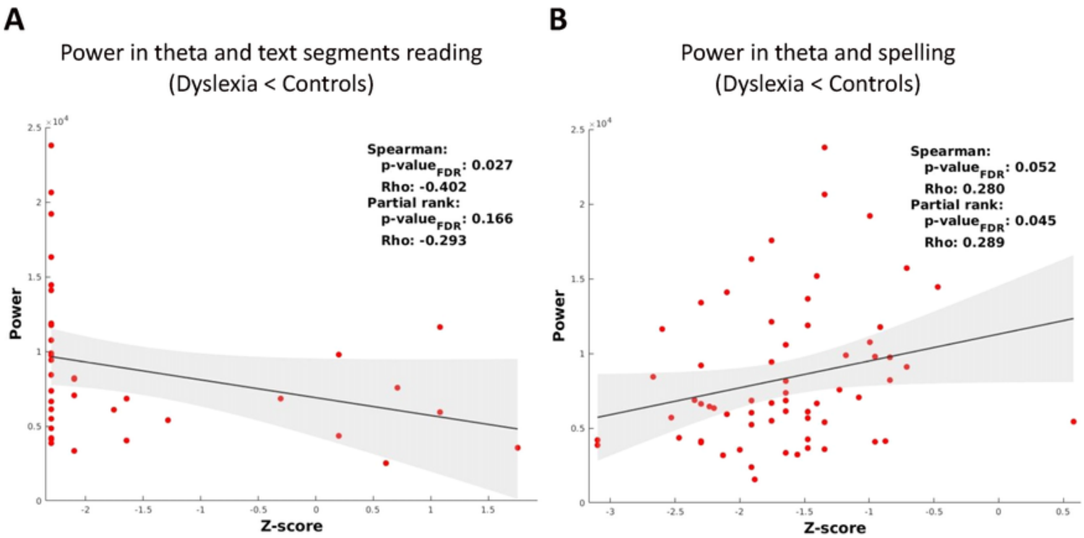

Figure 5

Significant correlations between averaged power from 261 left hemisphere in-mask vertices and cognitive performance. Results of Spearman and partial rank correlations between **A** power in theta band and text segments reading (n=37), and **B** power in theta band and spelling (n=63). p-values were FWE corrected. The grey strips represent 95% confidence intervals.

Supplementary Files

This is a list of supplementary files associated with this preprint. Click to download.

- SupplementaryTable1.xlsx
- SupplementaryFigure1.pdf
- SupplementaryFigure2.pdf
- SupplementaryFigure3.pdf